INTERNATIONAL JOURNAL OF COMMUNICATION SYSTEMS, VOL. 9, 35-45 (1996)

IMPACT OF BUSY LINES AND MOBILITY ON CALL BLOCKING IN A PCS NETWORK

YI-BING LIN AND WAI CHEN

Department of Computer Science and Information Engineering, National Chiao Tung University, Hsinchu, Taiwan, R.O.C.

SUMMARY

Several analytical models have been proposed to study the blocking probability for personal communications service networks or mobile phone networks. These models cannot accurately predict the blocking probability because they do not capture two important features. First, they do not capture the busy-line effect. Even if a cell has free channels, incoming and outgoing calls must be dropped when the destination portable is already in a conversation. Second, they do not capture the mobility of individual portables. In these models, mobility is addressed by net hand-off traffic to a cell, which results in traffic with a smaller variance to a cell compared with the true situation. We propose a new analytic model which addresses both the busy-line effect and individual portable mobility. Furthermore, our model can be used to derive the portable population distribution in a cell. The model is validated against the simulation experiments. We indicate that the previously proposed models approximate a special case of our model where the number of portables in a cell is 40 times larger than the number of channels.

KEY WORDS: blocking probability; handoff; mobility; personal communications

1. INTRODUCTION

In a *personal communcations services* (PCS) network, the total number of voice radio channels available is limited. Thus, the channels are reused for different conversations, in locations that are sufficiently distant from each other so that their transmissions do not interfere with one another. The service area is partitioned into *cells*, and a cell signifies the area in which a particular transmitter site is likely to serve *portable* (i.e., *mobile phone*) calls. To avoid interference, the channels are partitioned into several *channel sets*, and every channel set is nominated at exactly one cell, which cannot be used by other cells within the interference distance. Consider a cell with c channels. Assume that in the steady state, N customers are in the cell on the average and the incoming calls to a portable are a Poisson process with rate λ. The holding time for a call has an exponential distribution with rate μ. Several analytic models[1-4] have been proposed to study call blocking (new call blocking and hand-off call forced termination). In these models, the call arrivals are represented by two aggregated traffics: the net new call attempts and the net hand-off calls. In References 1 and 2, the net hand-off call arrival rate is derived by using the net new call rate and some mobility models. In References 3 and 4, both new call rate and hand-off call rate are given input parameters. The aggregate call arrivals imply that there is an infinite number of portables in a cell, and every call arrival is for a different portable in the cell. Such models have two problems:

1. These models do not capture the *busy-line effect.* Even if a cell has free channels, incoming and outgoing calls must be dropped when the destination portable is already in a conversation. The aggregate call arrivals do not consider individual portable behavior, and the models assume that a call is always connected if there is a free channel.
2. These models do not capture the mobility of *individual portables.* Suppose that the call arrival rate to a portable is λ, and there are N portables in a cell on the average. The previously proposed models ignore the notation N, and simply consider the net call arrival rate $N\lambda$. When a portable moves in or out of a cell, the net call arrival rate does not change. This approach does not reflect the real situation. For example, suppose that there are 10 portables in a cell at time t. Then the net call arrival rate to the cell is 10λ. If a portable moves in or move out of the cell at $t + \delta$, the net call arrival rate increases or decreases by 10 per cent instantaneously. In other words, assuming the net call arrivals as a Poisson process with a fixed rate is not appropriate.

An open queue model[5] has been proposed to address the mobility of individual portables. Unfortunately, three major equations (2), (4) and (5) in Reference 5 are not consistent, and the results may not be correct. Although the model considered the average number of portables in a cell, the net new call stream and the hand-off stream (see (4) and (5) in Reference 5) were used just like the other models,[2] and the effect of individual portable mobility was

CCC 1074-5351/96/010035-11

Received 24 August 1995
Revised 5 August 1995

not well treated. Furthermore, the busy-line effect was not considered in this model.

This paper proposes an analytical model to capture both the busy line effect and the individual portable mobility. Our model can also be used to derive the distribution of the portable population in a cell. The model is validated against the simulation experiments. We show that the previously proposed models approximate a special case (i.e., when $N \rightarrow \infty$) of our model. When N is not sufficiently large, the previously proposed models underestimate the blocking probability p_b (new call blocking and hand-off call forced termination) for a small offered load because the individual portable movement feature is not captured, and overestimate p_b for a large offered load because the busy-line effect is not captured.

2. THE BUSY-LINE EFFECT

This section models the busy-line effect by ignoring the mobility of portables (the mobility will be considered in the next section). That is, we assume that there are c channels and $N > c$ portables in a cell and no portable moves in or out of the cell. (Note that by ignoring the mobility, the hand-off stream does not exist, and the previously proposed model[1-4] degenerates into an Erlang-B system with a state diagram shown in Figure 1 (a).)

Let π_i be the steady state probability that i channels are busy. The state diagram of the used channels which captures the busy-line effect is given in Figure 1 (b). In this model, *state i* represents that i channels are in use, and a transition from state i to state $i+1$ is with rate $(N-i)\lambda$ for $i < c$. This transition implies that if i portables are busy in the cell, then the incoming (outgoing) calls to (from) these busy portables are dropped immediately and do not consume any free channels. Several measures are defined for the busy-line model. Let n_C be the number of incoming calls, n_A be the number of completed calls, n_D be the number of lost calls because of busy lines, and n_L be the number of lost calls because no channel is available. It is clear that

$$n_C = n_A + n_D + n_L \tag{1}$$

The ratio of the *effective call arrival rate per portable* is defined as

$$\lambda_e = \frac{n_C - n_D}{n_C}\lambda$$

Note that to improve the performance of a PCS network, λ_e should be considered to determine the number of channels, not λ. Let p_b be the blocking probability and p_b^* be the blocking probability which excludes the dropped calls caused by the busy-line effect (this probability is referred to as the *effective blocking probability*). That is,

$$p_b = \frac{n_L}{n_C}, \text{ and } p_b^* = \frac{n_L}{n_C - n_D} \tag{2}$$

Note that for the Erlang-B system, $p_b = p_b^*$ is expressed by the Erlang-B equation. In the busy-line model, $p_b \neq p_b^* = \pi_c$. Let x be the expected number of incoming calls arriving during one conversation. Then

$$n_D = x n_A$$

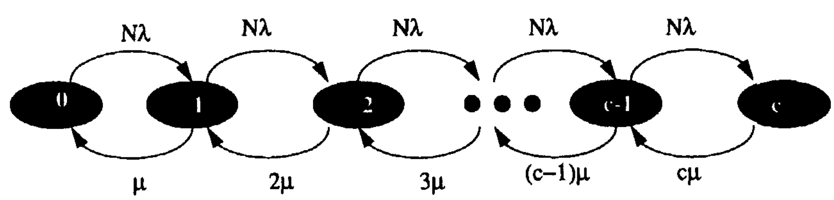

(a) The state diagram of the used channels (exclude the busy line effect)

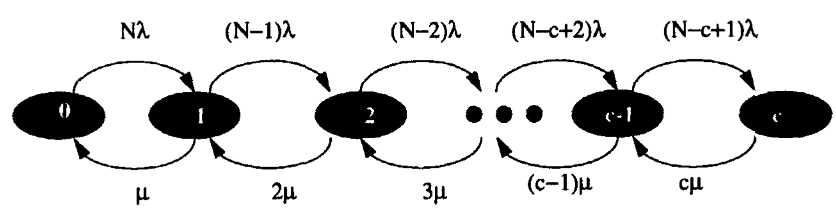

(b) The state diagram of the used channels (include the busy line effect)

Figure 1. The state diagram for the number of used channels

Figure 2 illustrates the case when i calls are dropped during a conversation. Let $t' = t_0 + t_1 + \ldots + t_{i-1}$. Because the incoming calls form a Poisson process with rate λ and the holding times have an exponential distribution with mean $1/\mu$, we have

$$\begin{aligned} x &= \sum_{i=1}^{\infty} i\Pr[t' \le t < t' + t_i] \\ &= \sum_{i=1}^{\infty} i \int_{t=0}^{\infty} \int_{t'=0}^{t} \int_{t_i=t-t'}^{\infty} \mu e^{-\mu t} \frac{(\lambda t')^{i-1}}{(i-1)!} \lambda e^{-\lambda t'} \lambda e^{-\lambda t_i} dt_i dt' dt \\ &= \sum_{i=1}^{\infty} \frac{i\lambda^i \mu}{(\lambda+\mu)^{i+1}} \\ &= \frac{\lambda}{\mu} \end{aligned} \quad (3)$$

Thus

$$n_D = \frac{\lambda n_A}{\mu} \quad (4)$$

From (1), (2) and (4), we have

$$p_b = \frac{p_b^*}{1 + (1-p_b^*)\left(\frac{\lambda}{\mu}\right)} \quad (5)$$

Let p_a be the probability that a call is completed (i.e., accepted) and p_d be the probability that a call is dropped because of the busy-line effect, then

$$p_a = \frac{n_A}{n_C} = \frac{1-p_b^*}{1 + (1-p_b^*)\left(\frac{\lambda}{\mu}\right)} \quad (6)$$

$$p_d = \frac{n_D}{n_C} = x p_a = \frac{(1-p_b^*)\left(\frac{\lambda}{\mu}\right)}{1 + (1-p_b^*)\left(\frac{\lambda}{\mu}\right)} \quad (7)$$

and

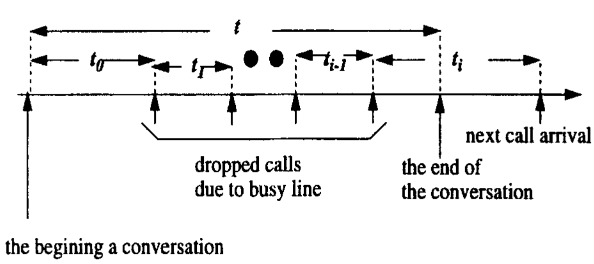

Figure 2. Calls lost as a result of the busy line

$$\lambda_e = \lambda(1-p_d) = \frac{\lambda}{1 + (1-p_b^*)\left(\frac{\lambda}{\mu}\right)} \quad (8)$$

The probability p_b^* (i.e., π_c) is derived by considering the state diagram in Figure 1 (b). For $1 \le i \le c$, we have[6]

$$\pi_i = \frac{(N-i+1)\lambda}{i\mu} \pi_{i-1} = \frac{\lambda^i \prod_{j=1}^{i} (N-i+1)}{i!\mu^i}$$

$$\pi_0 = \binom{N}{i}\left(\frac{\lambda}{\mu}\right)^i \pi_0 \quad (9)$$

From (9) and the fact that $\pi_0 + \pi_1 + \ldots + \pi_n = 1$, we have

$$p_b^* = \pi_c = \frac{\binom{N}{c}\left(\frac{\lambda}{\mu}\right)^c}{\sum_{0 \le i \le c} \binom{N}{i}\left(\frac{\lambda}{\mu}\right)^i} \quad (10)$$

Figure 3 (a) illustrates the impact of the busy-line effect. In the figure, $c = 10$. Two sets of curves are considered. The dashed curves are for $N = 200$, and the solid curves are for $N = 20$. In each set of curves, the curve marked o plots the Erlang-B equation, the curve marked • plots equation (5) for the busy-line model, and the curve marked * plots the simulation results (the simulation setup will be discussed in Section 5). Figure 3 (a) indicates that the busy-line model is consistent with the simulation study. We observe that when N is small, Erlang-B is not appropriate to predict call blocking for a PCS network with low mobility. Figure 3 (b) plots λ_e against λ. When the number of portables in a cell is small, every portable is likely to connect for the first phone call, and the subsequent incoming calls are likely to be blocked as a result of the busy-line effect. Thus, the effective arrival rate per portable is small. When N is large, it is more likely that a portable is unable to connect to any incoming call (because there is no free channel), and the busy-line effect is less significant, and the effective rate λ_e approaches λ.

3. THE MOBILITY MODEL

This section considers the portable mobility as well as the busy-line effect. We assume that in the steady state, there are N portables in a cell on average. Besides the parameters defined in the busy-line model, two parameters λ_m and α are introduced. Suppose that the time a portable resides in a cell has an exponential distribution with the expected time $1/\lambda_m$. The portable moves to the neighbouring cells with the same probabilities. Thus, in the steady state, the rate λ_E at which portables move to a cell

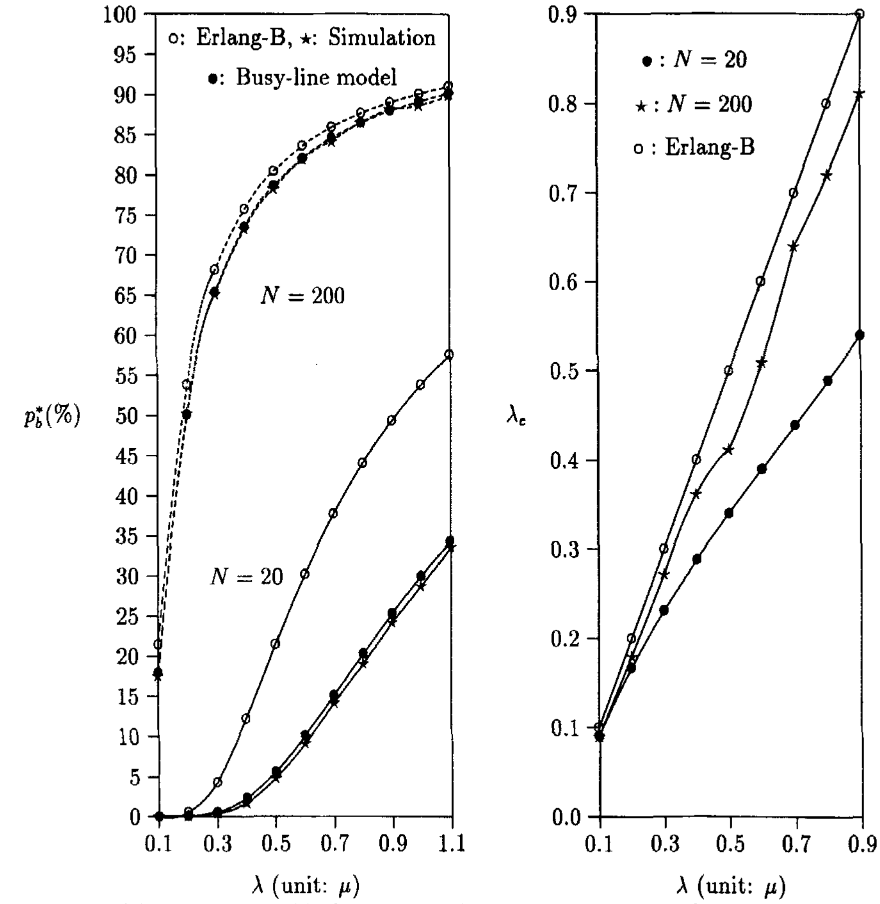

(a) The effective blocking probability (b) The effective arrival rate

Figure 3. The impact of the busy-line effect on the effective blocking probability (c = 10. Dashed curves: N = 200; solid curves: N = 20; o: the Erlang-B system; •: the busy-line model: *: simulation)

equals the rate at which portables move out of the cell, where

$$\lambda_E = N\lambda_m$$

Another parameter, α, represents the probability that a hand-off occurs when a portable moves in a cell. In the mobility model, a state is a pair (i,j) where i represents the number of used channels $(0 \leq i \leq c)$, and j represents the number of portables in the cell $(i \leq j \leq \infty$; note that the number of portables is no less than the number of used channels). Figure 4 illustrates the transitions for state (i,j). The Markov process moves from state (i,j) to $(i,j+1)$ if a new portable not in a conversation arrives at the cell (and no hand-off occurs) when there are i used channels and j portables in the cell. The transition rate is $(1-\alpha)\lambda_E$. The Markov process moves from state $(i,j+1)$ to (i,j) if a portable not in a conversation leaves the cell. Since there are $(j-i+1)$ portables not in a conversation, the transition rate is $(j-i+1)\lambda_m$. The Markov process moves from state (i,j) to $(i+1, j+1)$ if a new portable in conversation arrives at the cell (and a hand-off occurs) when there are i used channels and j portables in the cell. The transition rate is $\alpha\lambda_E$. The Markov process moves from state $(i+1,j+1)$ to (i,j) if a portable in a conversation leaves the cell. Because there are $(i+1)$ portables in a conversation, the transition rate is $(i+1)\lambda_m$. The Markov process moves from state (i,j) to $(i+1,j)$ if an incoming call arrives for a portable not in conversation. The transition rate is $(j-i)\lambda$. The Markov process moves from state $(i+1,j)$ to (i,j) if a portable completes a conversation. The transition rate is $(i+1)\mu$. The complete state diagram is given in Figure 5. The probability $\pi_{i,j}$ that the

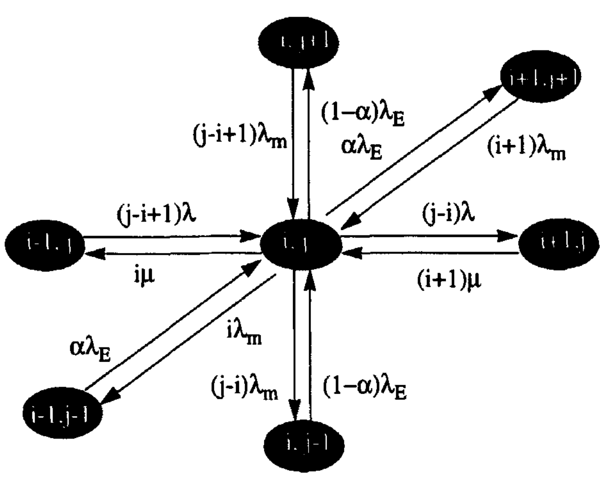

Figure 4. The transitions for state (i,j)

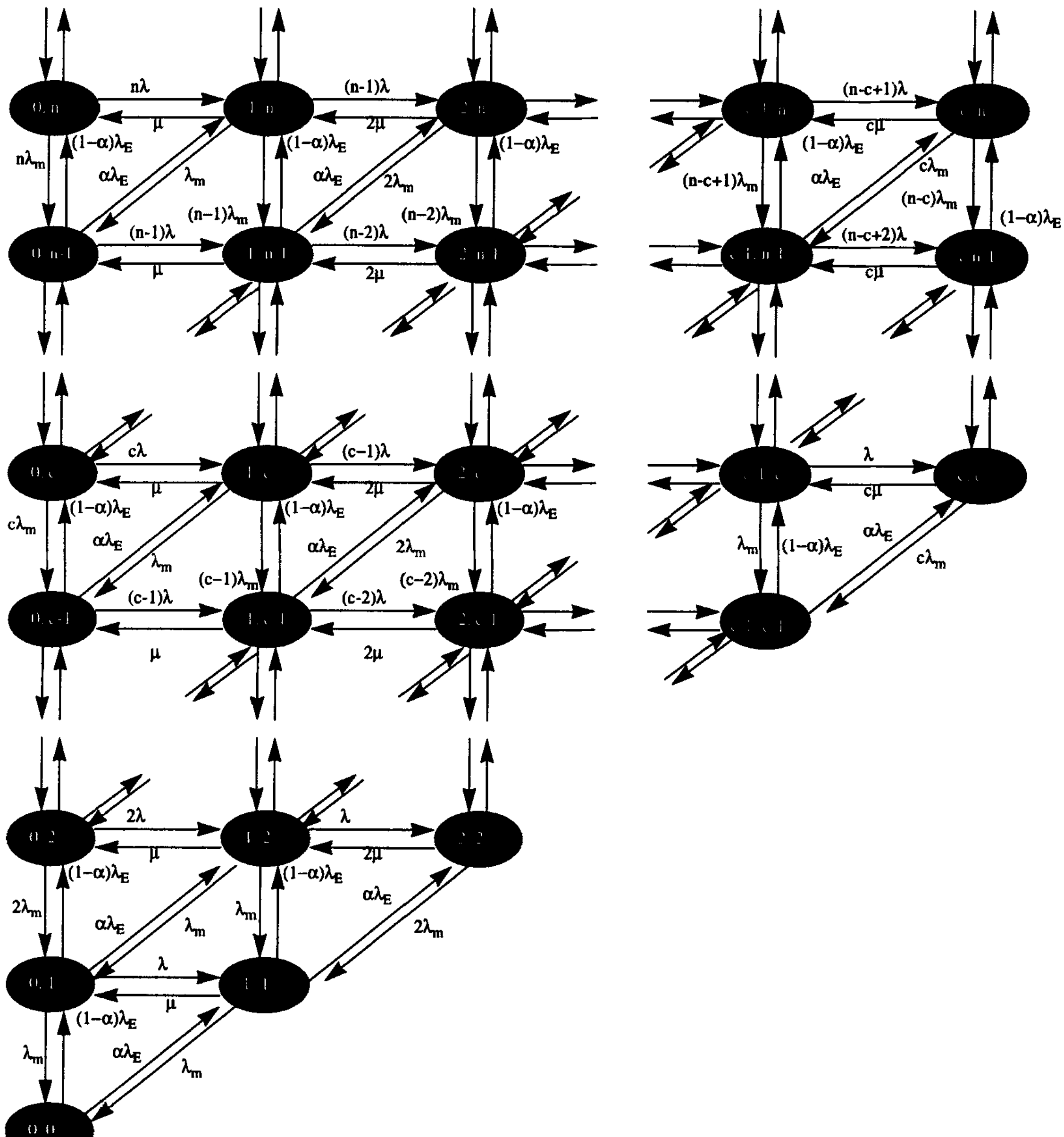

Figure 5. The state diagram for the mobility model

Markov process is in state (i,j) is given below. For $0 < i < c$ and $j > 0$,

$$\pi_{i,j} = \frac{1}{\lambda_E + (j-i)\lambda + j\lambda_m + i\mu} [(j-i+1)(\lambda_m \pi_{i,j+1} + \lambda \pi_{i-1,j}) + (i+1)(\lambda_m \pi_{i+1,j+1} + \mu \pi_{i+1,j}) + (1-\alpha)\lambda_E \pi_{i,j-1} + \alpha \lambda_E \pi_{i-1,j-1}] \quad (11)$$

For $i = 0$ and $j > 0$,

$$\pi_{0,j} = \frac{(j+1)\lambda_m \pi_{0,j+1} + \lambda_m \pi_{1,j+1} + \mu \pi_{1,j} + (1-\alpha)\lambda_E \pi_{0,j-1}}{\lambda_E + j\lambda + j\lambda_m}$$

For $i = c$ and $j > 0$,

$$\pi_{c,j} = \frac{1}{(1-\alpha)\lambda_E + j\lambda_m + c\mu} [(j-c+1)\lambda_m \pi_{c,j+1} + (1-\alpha)\lambda_E \pi_{c,j-1} + \alpha\lambda_E \pi_{c-1,j-1} + (j-c+1)\lambda \pi_{c-1,j}] \quad (13)$$

For $0 < i = j < c$,

$$\pi_{i,j} = \frac{\lambda_m \pi_{i,i+1} + (i+1)\lambda_m \pi_{i+1,i+1} + \alpha\lambda_E \pi_{i-1,i-1} + \lambda \pi_{i-1,i}}{\lambda_E + i\lambda_m + i\mu} \quad (14)$$

For $i = j = c$,

$$\pi_{c,c} = \frac{\lambda_m \pi_{c,c+1} + \alpha\lambda_E \pi_{c-1,c-1} + \lambda \pi_{c-1,c}}{(1-\alpha)\lambda_E + c\lambda_m + c\mu} \quad (15)$$

For $i = j = 0$,

$$\pi_{0,0} = \frac{\lambda_m(\pi_{0,1} + \pi_{1,1})}{\lambda_E} \tag{16}$$

The probability α is derived as follows. Assume that $\lambda_m << \lambda$ and consider the last conversation of a portable before it leaves the cell. Figure 6 gives the timing diagram when a hand-off occurs. The incoming calls form a Poisson process, and $t_1, t_2, \ldots, t_{i-1}$ have the same exponential distribution. Since the time that a portable resides in a cell is exponentially distributed, the time when the portable leaves the cell is a random observer of the incoming call process and the residual time t_0 also has the same distribution as t_j $(1 \le j < i)$. Thus, let $t' = t_0 + t_1 + \ldots + t_{i-1}$,

$$\begin{aligned}
\alpha = \Pr[t > t'] &= \sum_{i=1}^{\infty} \Pr[t > t' \text{ and } t' = t_0 + \ldots + t_{i-1}] \\
&= \sum_{i=1}^{\infty} \Pr[t > t']\Pr[t' = t_0 + \ldots + t_{i-1}] \\
&= \sum_{i=1}^{\infty} \left[\int_{t=0}^{\infty} \mu e^{-\mu t} \int_{t'=0}^{t} p_a p_d^{i-1} \frac{(\lambda t')^{i-1}}{(i-1)!} \lambda e^{-(\lambda t')} dt' dt \right] \\
&= \sum_{i=1}^{\infty} \left\{ \int_{t=0}^{\infty} \mu e^{-\mu t} \left(\frac{\lambda}{\mu}\right)^{i-1} p_a^i \left[1 - \sum_{j=0}^{i-1} \frac{(\lambda t)^j}{j!} e^{-(\lambda t)} \right] dt \right\} \\
&= \sum_{i=1}^{\infty} \left[\left(\frac{\lambda}{\mu}\right)^{i-1} p_a^i - \left(\frac{\lambda}{\lambda+\mu}\right)^{i-1} p_a^{i-1} \sum_{j=0}^{i-1} \left(\frac{\lambda}{\lambda+\mu}\right)^j \right] \\
&= \frac{\left(\frac{\lambda}{\mu}\right) p_a}{1 + \left(\frac{\lambda}{\mu}\right) - \left(\frac{\lambda}{\mu}\right)^2 p_a}
\end{aligned} \tag{17}$$

The probabilities $\pi_{i,j}$ are computed numerically by a two-level iterative procedure. Note that the state space for the mobility model is infinite (because $i \le j \le \infty$). In order to compute $\pi_{i,j}$ numerically, we select a number, N_*, such that $i \le j \le N_*$. In the procedure, we iterate by increasing N_* until the output measure converges. Let $N_*(m)$ be the value chosen in the mth iteration. In this iteration, the probabilities $p_{i,j}$, p_b^* and α are also computed iteratively. Let $\pi_{i,j}(k,m)$, $p_b^*(k,m)$, and $\alpha(k,m)$ be the values computed in the kth inner iteration when $N_* = N_*(m)$. The procedure is described below.

Step 1. $N_*(0) \leftarrow N_0$, $m \leftarrow 0$, $p_b^*(0) \leftarrow 0$. (In this paper, $N_0 = 1000$.)

Step 2. For $0 \le i \le c, i \le j \le N_*(m)$,

$$p_{i,j}(0,m) \leftarrow \frac{i}{0.5(c+1)(c+2) + (c+1)N_*(m)}$$

$$p_b^*(0,m) \leftarrow \sum_{c<j<N_*(m)} \pi_{c,j}(0,m)$$

$$\alpha(0,m) \leftarrow 0 \text{ and } k \leftarrow 1$$

Step 3. Compute $\pi_{i,j}(k,m)$ using equations (11)–(16), and the state probabilities computed in the previous iteration.

Step 4. $p_b^*(k,m) \leftarrow \sum_{c<j<N_*(m)} \pi_{c,j}(k,m)$.

Step 5. Compute $\alpha(k,m)$ using $p_b^*(k,m)$ and equations (6) and (17).

Step 6. If the difference of $\pi_{c,j}(k,m)$ and $\pi_{c,j}(k,m-1)$ is larger than a threshold for all $c \le j \le N_*(m)$, then $k \leftarrow k+1$ and go to Step 3.

Step 7. If the difference of $p_b^*(m) = p_b^*(m,k)$ and $p_b^*(m-1)$ is larger than a threshold then $N_*(m) \leftarrow N_*(m-1) + \delta$ and go to Step 2. (In this paper, $\delta = 10$).

Although we do not have proof of the convergence of the procedure, it does converge for all experiments studied in this paper.

Figure 7 plots p_b^* for the mobility model for $c = 8$ and $N = 80$. The solid curves represent $\lambda_m = 0.02\mu$. The dashed curves represent $\lambda = 0.01\mu$. The plain curves represent the analytical results. The curves marked o represent simulation. In these two sets of experiments, the procedure converges at $N_* < 4000$ in all cases. Figure 7 indicates that the mobility model is consistent with the simulation study.

Our model can also be used to derive the distribution of the portable population in a cell. Consider the state diagram in Figure 5. Let π_i be the steady state probability that there are i portables in a cell. Then $P_i = \sum_{0 \le j \le i} p_{j,i}$. If we only consider the aggregate probability π_i, then the model degenerates into an $M/M/\infty$ queue with arrival rate λ_E and completion rate λ_m. From the standard technique,[6]

$$P_i = \frac{N^i e^{-N}}{i!} \tag{18}$$

Figure 8 plots (18) and validates the equation against the simulation experiments. The population distribution has been used to study portable registration and deregistration for a PCS network.[7]

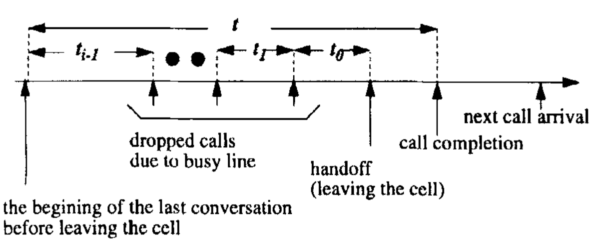

Figure 6. The timing diagram when a hand-off occurs

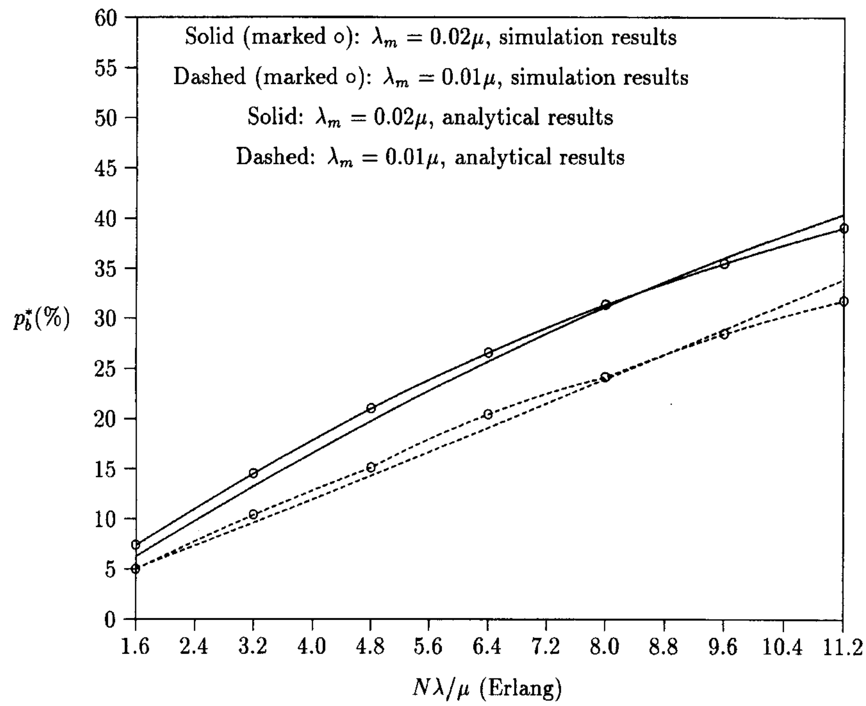

Figure 7. The probability p_b^* against λ (N = 80)

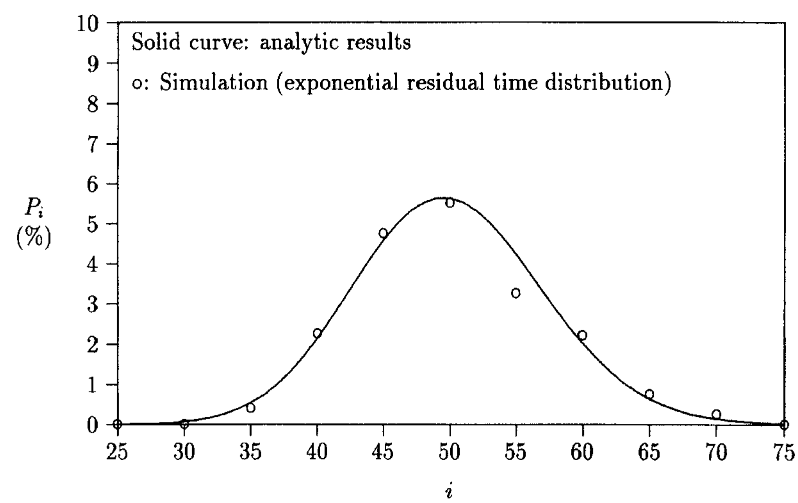

Figure 8. The population distribution (N = 50)

4. SIMULATION

This section presents the simulation results. To simulate a very large PCS network, we proposed a wrap-around hexagonal topology for simulation.[8] This approach eliminates the boundary effect which occurs in an un-wrapped topology. Study indicated that the wrapped topology yields better accuracy with less computing resources compared with the un-wrapped topology (to achieve the same output accuracy for a 37-node wrapped topology, at least 169 nodes are required in an un-wrapped topology). An 8 × 8 wrapped mesh topology is considered in this paper (see Figure 9). The mobility behaviour of portables in the simulation is described by a two-dimensional random walk proposed in Reference 9. In this model, a portable stays in a cell for a period of time which has an exponential distribution with mean $1/\lambda_m$. Then the portable moves to one of the four neighbouring cells with the same routing probabilities 0.25. Initially, every cell has N = 80 portables. Four hundred thousand incoming calls are simulated to ensure that the confidence interval of the 95 per cent confidence level of p_b^* is less than 3 per cent of the mean value $E[p_b^*]$. Figures 10 and 11 plot p_b, p_a, p_d, and α against λ. In these figures, c = 8, N = 80, λ_m = 0.01μ and 0.02μ. Figure 10 (a) plots p_b for λ_m = 0.01μ, λ_m = 0.02μ, and Erlang-B. Figure 10 (b) plots p_a against λ. The figure indicates that by doubling the mobility from 0.01μ to 0.02μ, the call completion probability dropped from 1 per cent to 7 per cent when λ increases from 0.1μ to 0.7μ. Figure 11 (a) plots p_d against λ. The probability p_d decreases as the

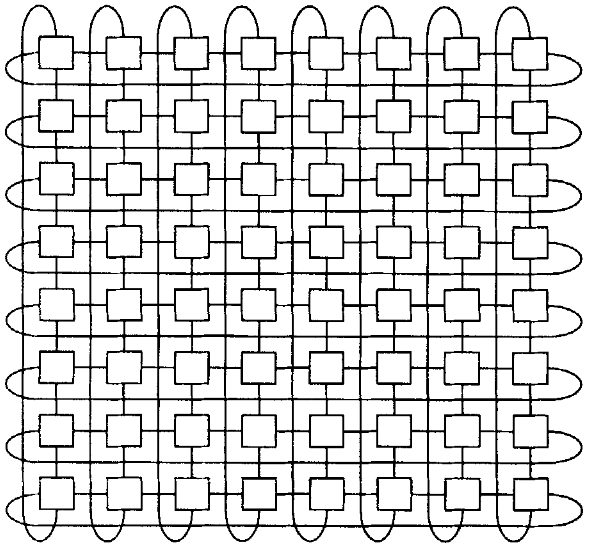

Figure 9. The PCS network topology considered in the simulation

mobility increases. This phenomenon is similar to the behaviour of λ_e described in the busy-line model. Increasing the mobility has the effect of increasing the randomness of the incoming call traffic to a cell, which has the similar effect of increasing the portable population in the busy-line model. Note that p_a and p_d measured from the simulations are consistent with the equation

$$p_d = \frac{\lambda p_a}{\mu}$$

derived in our analytical model (see Equation (3)). For example, consider $\lambda = 0.7\mu$, $\lambda_m = 0.01\mu$, and $p_a = 0.4456$. From the simulation, $p_d = 0.3107$ (see Figure 11 (a)), and from the analytical analysis, $p_d = 0.3112$, figure 11 (b) plots α, the probability of hand-off, against λ. Note that when λ is large (e.g., $\lambda > 0.4$), changing the λ value does not have a significant impact on α as when λ is small (e.g., $\lambda < 4$). The α values measured from the simulations are consistent with equation (17) derived from our analytical model (see Figure 11 (b)).

Figure 12 shows the impact of N (where $\lambda_m = 0.25\mu$ and $c = 5$). In Figure 12 (a), p_b^* for a PCS system with a small N is much larger than a PCS system with a large N. This phenomenon is caused by the mobility of individual portables (p_b^* is not directly affected by the busy-line effect because the drops as a result of busy lines are excluded from this measure). For a small N, a portable movement will significantly change the net call arrival rate to a cell. In other words, the individual portable moment effect significantly increases the variance of call arrival rate to a cell for a small N. In Figure 12 (b), p_b is affected by the individual portable

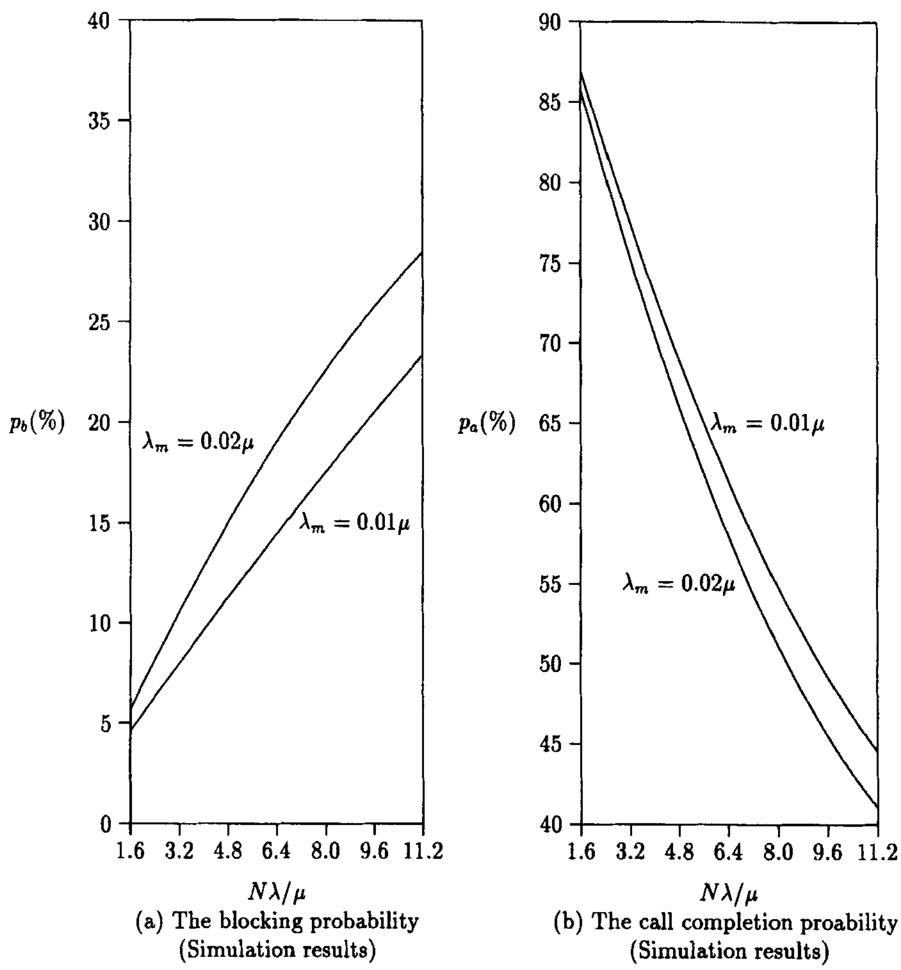

Figure 10. The probabilities p_b and p_a

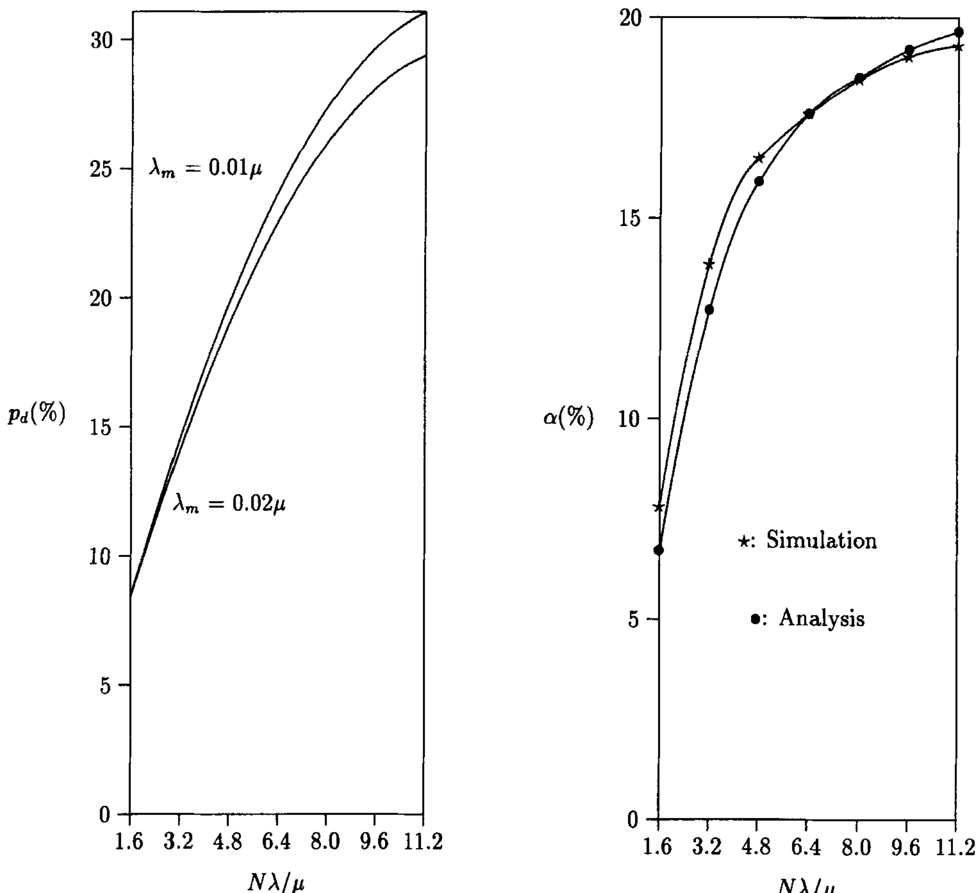

(a) Blocking due to busy line (Simulation results)

The handoff probability

Figure 11. The probabilities p_d and α

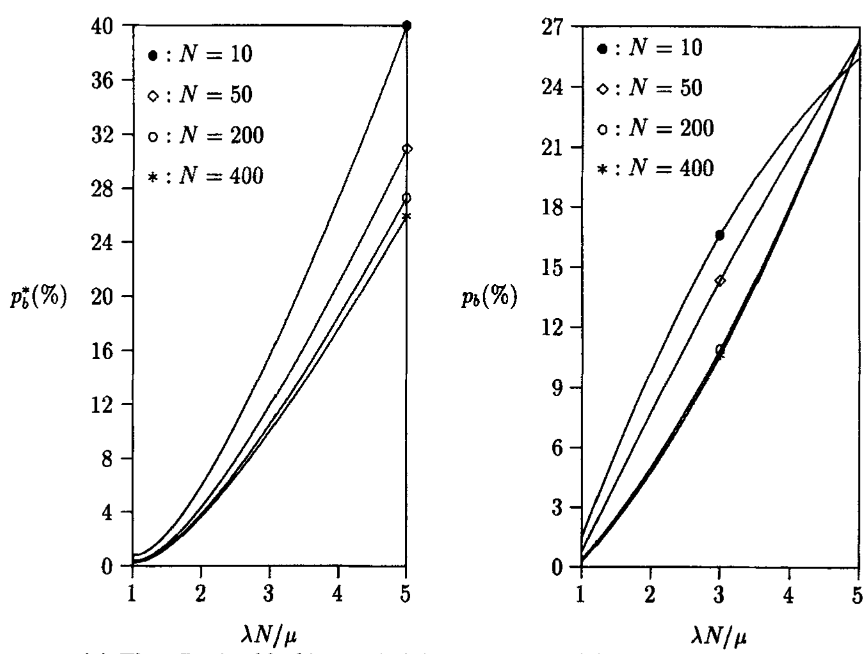

(a) The effective blocking probability

(b) The blocking probability

Figure 12. The effect of N ($\lambda_m = 0.25\mu$, $c = 5$)

movement when the offered load ($\lambda N/\mu$) is small (and p_b for a small N is larger than p_b for a large N, as explained above). When the offered load is large (e.g., $\lambda N/\mu > 4.8$ in Figure 12 (b)), p_b for a small N is smaller than p_b for a large N. This phenomenon is explained as follows. For the same (large) offered load, the call arrival rate to a portable is larger for a smaller N, and more calls are dropped as a result of busy lines. These dropped calls do not contribute to the numerator of p_b (note that the busy lines are counted in the denominator). On the other hand, when N is very large, the call arrival rate to a portable is small. Thus, the busy-line effect is insignificant, and most call arrivals should be connected if there are free channels. In other words, the effective call arrivals are not reduced by the busy-line effect for a large N. The consequence is that the probability that all channels are busy increases, and p_b is large compared with the case when N is small. Note that $p_b^* >> p_b$ for $N < 50$ and $p_b^* \simeq p_b$ for $N > 400$. In other words, the busy-line effect can be ignored only if the number of portables is much larger than the number of channels. Theoretically, the p_b curves for the previously proposed models[1-4] approaches our model when $N \rightarrow \infty$. Figure 12 indicates that these models are appropriate only if N is 40 times larger than c. If N is not sufficiently large, the previously proposed models underestimate p_b for a small offered load, and overestimate p_b for a large offered load. The previously proposed models always underestimate p_b^*.

5. CONCLUSIONS

Several analytical models[1-4] have been proposed to study the blocking probability of a PCS network. These models consider an aggregate new call arrival stream to a cell. The portable mobility is modelled by an extra aggregate hand-off call arrival stream to the cell. These models do not capture two important features of a PCS network: the busy-line effect and the movement of individual portables. This paper proposed a new analytical model to address these two features by considering N, the average number of portables in a cell as an input parameter. With this input parameter, we have also derived the distribution of the portable population in a cell. The model was validated against the simulation experiments. Our study indicated that the previously proposed models approximate a special case (i.e., $N \rightarrow \infty$) of our model. When N is not sufficiently large, the previously proposed models underestimate the blocking probability p_b (new call blocking and hand-off call forced termination) for small offered load because the individual portable movement feature is not captured; and overestimate p_b for a large offered load because the busy-line effect is not captured.

REFERENCES

1. G. J. Foschini, B. Gopinath and Z. Miljanic, 'Channel cost of mobility', *IEEE Trans. Veh. Technol.*, **42** (4), 414–424 (1993).
2. D. Hong and S. S. Rappaport, 'Traffic model and performance analysis for cellular mobile radio telephone systems with prioritized and no-protection handoff procedure', *IEEE Trans. Veh. Technol.*, **VT-35** (3), 77–92 (1986).
3. S. Tekinary and B. Jabbari, 'A measurement based prioritization scheme for handovers in cellular and microcellular networks', *IEEE J. Select. Areas Commun.*, 1343–1350 (October 1992).
4. C. H. Yoon and K. Un, 'Performance of personal portable radio telephone systems with and without guard channels', *IEEE J. Select. Areas Commun.*, **11** (6), 911–917 (1993).
5. D. McMillan, 'Traffic modelling and analysis for cellular mobile networks', *ITC-13*, 1991, pp. 627–632.
6. L. Kleinrock, *Queueing Systems. Vol. 1 – Theory*. Wiley, New York, 1976.
7. Y. -B. Lin and A. Noerpel, 'Implicit Deregistration in a PCS Network', *IEEE Trans. Veh. Technol.*, **43** (4), 1006–1010 (1994).
8. Y. -B. Lin and V. K. Mak, 'Eliminating the boundary effect of a large-scale personal communication service network simulation', *ACM Trans. on Modeling and Computer Simulation*, **4** (2), 165–190 (1994).
9. Y. -B. Lin, 'Performance modeling of location forwarding in a PCS network', Technical Report TM-ARH-022891, Bellcore, 1993.

Authors' biographies:

Yi-Bing Lin received his B.S.E.E. degree from National Cheng Kung University in 1983, and his Ph.D. degree in computer science from the University of Washington in 1990. Between 1990 and 1995, he was with the applied research area at Bell Communications Research (Bellcore), Morristown, NJ. In 1995, he was appointed full professor of the Department and Institute of Computer Science and Information Engineering, National Chiao Tung University. His current research interests include the design and analysis of personal communications services networks, distributed simulation and performance modelling. He is a subject area editor of the *Journal of Parallel and Distributed Computing*, an associate editor of the *International Journal in Computer Simulation*, an associate editor of *SIMULATION* magazine, a member of the editorial board of the *International Journal of Communications* and a member of the editorial board of *Computer Simulation Modeling and Analysis*. He is also Program Chair for the 8th Workshop on Distributed and Parallel Simulation, and General Chair for the 9th Workshop on Distributed and Parallel Simulation.

Wai Chen received his B.S. degree from Zhejiang University, Zhejiang, China, and his M.S., M.Phil. and Ph.D. degrees from Columbia University, New York; all in electrical engineering. From 1984 to 1989, he was a graduate research assistant at the Center for Telecommunications Research (CTR) at Columbia University, where he carried out research in the design and evaluation of integrated services protocols. He joined SBC Technology Resources in 1989, where he was a senior technologist in the advanced network technology group, responsible for the analysis of next-generation switching systems. Since

1992, he has been a research scientist at the applied research organization of Bell Communications Research (Bellcore). He has been, since March 1993, Bellcore's principal investigator (PI) of an ARPA-funded project on bandwidth management and access control for B-ISDN. His current research interests include resource management of wireless ATM access networks, mobile connection admission and dynamic traffic control in mixed wireless and wireline networks, and B-ISDN traffic management. He is a member of the IEEE, sigma Xi, and the Mathematical Association of America.